



Formation and growth of NbSe₃ topological crystals

T. Tsuneta*, S. Tanda

Department of Applied Physics, Hokkaido University, Sapporo 060-8628, Japan

Received 14 October 2003; accepted 2 December 2003

Communicated by T. Hibiya

Abstract

We investigated the self-assembled growth of μm -scale topological crystals of NbSe₃ based on the chemical vapor transportation method. The shapes of these materials, including cylinders, Möbius strips and “figure-eight” strips, are the physical realization of topological configurations defined by wedge and twist disclinations as well as dispirations. The crystal structure is investigated by X-ray powder diffraction technique and it is revealed that they are NbSe₃ crystals with a considerable strain. The variations in topology and growth form (e.g. rings, disks and tubes) are explained based on a growth model that a NbSe₃ whisker encircles a selenium droplet by the surface tension to form a loop. The twisted topologies of Möbius strips and figure-eight strips originates from either the symmetry of the elastic property of NbSe₃ or bend-twist transformation.

© 2003 Elsevier B.V. All rights reserved.

PACS: 81.10.-h; 61.72.Lk

Keywords: A1. Crystal morphology; A1. Defects; A1. Growth models

1. Introduction

Controlling the global geometry of a material is now regarded as an important method for obtaining new materials. In particular, a topological deformation, such as the rolling of a planar crystal into a cylinder, can significantly affect physical properties via changes in spatial symmetry (rotational, translational and/or chiral symmetry). Such new materials include fullerenes [1] and related nested onion-like structures [2], carbon nanotubes [3] and various

inorganic tubular systems [2–6]. These are called topological materials because, in mathematical terms, the spherical surface (fullerene) and the cylindrical surface (nanotube) correspond to phase spaces S_2 and $S_1 \times I$, respectively. These multi-connected spaces are topologically different from the two-dimensional space R_2 of the original flat materials. They are useful for fundamental studies of both the physics of multi-connected geometries [7] as well as nano-physics, due to the reduction in size that accompanies the new topology. However, no topological materials other than originally two-dimensional layered crystals, like graphite, have been made into curved surfaces.

Recently, we developed the self-assembled growth of micrometer-scale NbSe₃ crystals that

*Corresponding author. Tel.: +81-11-706-7126; fax: +81-11-706-7293.

E-mail address: tsuneta@eng.hokudai.ac.jp (T. Tsuneta).

URL: <http://exp-ap.eng.hokudai.ac.jp>.

have various multi-connected geometries [8]. NbSe₃ is originally a quasi-one-dimensional material and its ordinary crystal shape is a whisker or a thin ribbon. These new geometries include rings, disks, tubes and two twisted versions of a cylinder: Möbius strips and “figure-eight” (8-) strips, which are characterized by twists of π and 2π , respectively. These are not simply hollow crystals carved out of a bulk material: their crystal axes are mapped onto the curved geometries. Thus these crystals form a new group of topological crystal of a one-dimensional material. They are remarkable examples of a μm -scale monocrystal with unlocalized, complete wedge and twist disclinations as well as dispirations. Aside from crystallography, it is interesting how the multi-connected topology affects the electronic properties of NbSe₃, especially its characteristic charge-density-wave (CDW) states [9–11].

A variety of crystal topologies under virtually the same conditions is a significant feature of this material. A variety of topological materials: untwisted rings, π -twisted Möbius strips and 2π -twisted 8strips can all be produced together in a single growth batch. In addition, there are further varieties within the same topological class, e.g. flat disks, fine tubes, paraboloids or more complex objects have the topology of a cylinder. In this paper, we focus on the mechanism of the self-assembled growth with this unusual morphology. We report the effects of the growth conditions on the morphology as well as structural properties of these materials as studied by X-ray diffraction, which are apparently related to their formation and growth.

2. Experiments

2.1. Sample preparation

Since the first report in 1975 [12], single crystals of NbSe₃ have been synthesized by the chemical vapor transportation (CVT) method [13,14]. We used this method to synthesize topological crystals and studied the effects of the experimental conditions on crystal morphology. Since we observed that strong convection of selenium (Se) vapor/mist

inside the reaction apparatus is crucial for the formation of topological crystals, we used a reaction furnace with inadequate insulation to induce a large thermal inequilibrium. We used niobium (Nb) in the form of either powder or rods and granular Se. Both elements were obtained in a purity of greater than 4N from the manufacturer. The starting material was a mixture of Nb and Se with about 3% excess Se as a transport agent. Nb and quartz ampoules were baked at around 900°C in a vacuum for degassification. Se was also degassed by boiling in vacuum. Nb rods were treated with a solution of hydrofluoric acid and nitric acid prior to baking. Shortly after baking, the mixture was sealed in a quartz ampoule, 1.75 mm in internal diameter and 20 cm in length, that was evacuated to the order of 10^{-6} Torr. The ampoule was placed horizontally in an open-end furnace with the starting material placed on the high-temperature side. The temperature of the starting-material end of the ampoule was raised to the reaction temperature, typically 740°C, at a rate of 10°C/min. A temperature gradient $-1.5^\circ\text{C}/\text{cm}$ was applied to the ampoule. The temperature was then maintained for 0.5–100 h before the ampoule is quenched.

2.2. Effects of growth conditions

Using the above procedure, we can reproducibly synthesize dozens of topological crystals, equivalent to a yield of around 10^{-3} wt%, along with NbSe₃ whisker. The growth region for topological crystals is always on the colder side of the ampoule. A certain growth stage of surrounding NbSe₃ whiskers seems to be crucial for the formation of topological crystals. Whiskers grown in the region are so fine and soft that most of them are rumpled. They also tend to radiate outward from several apparent growth points. Growth is likely to originate from Se droplets, since Se condenses into a liquid as it circulates around the ampoule as a transport agent. The growth region in the ampoule is typically 1–5 cm long in the case of powders. The temperature in this region is usually 710–720°C regardless of the maximum/minimum temperature at both ends.

Topological crystals are most efficiently produced within the first few hours of the reaction. Fig. 1 shows the yield (in number) of topological crystals for different reaction times, where the open and filled circles represent Nb powders and rods used as a starting material, respectively. In the case of powders, the formation of topological crystals starts within 60 min and gradually slows. After reaching a peak at 300–400 min, the yield begins to decrease, possibly due to decomposition. With Nb rods instead of powders, the yield of topological crystals is improved and they are produced for longer time. In addition, the growth region of topological crystals increases to 10–20 cm. A rod reacts with a Se atmosphere at a slower rate. While all of Nb powder is crystallized into NbSe₃ whiskers within 30 min, with a rod, more than 90% of the starting material remains unreacted after thousands of minutes. This difference is likely due to the greater surface area of Nb powders, where the reaction with Se gas takes place, and powder scattered on the wall of ampoule provides efficient nucleation centers for whiskers.

2.3. Classification of crystal topologies

The morphology of our topological crystals can basically be represented by a framed strip rolled

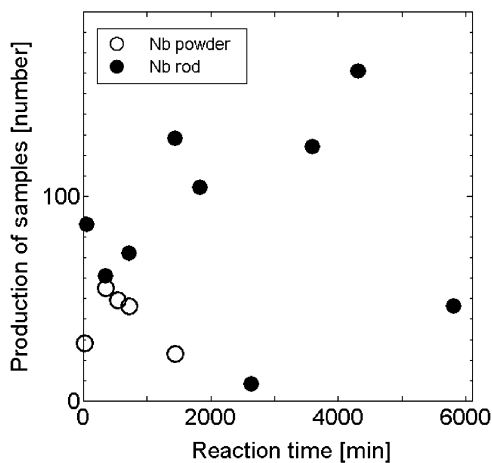


Fig. 1. Production rate of topological crystal samples picked from growth batches at different reaction times. Open and solid circles represent niobium as a starting material in the form of a powder and rod, respectively.

into a loop with or without a twist along its circumference. The morphology can be categorized into three classes according to the degree of twist: 0, π or 2π . Our classification is based on topology, i.e. each crystal belongs to a different class in the ribbon-knot group in terms of mathematics. The linking number lk is introduced to simply characterize all three classes. $lk = Wr + Tw$ according to White's theorem [15], where the writhing number Wr is derived from the angle of curvature of a ribbon integrated over the whole length, and the twisting number Tw is the integrated screw angle between the two edges of a ribbon. lk , Wr and Tw are invariants, so that originally they have integral values in units of 2π . However, since we must address π -twisted Möbius strips, half-integral numbers are also allowed. For the topology of a ring (cylinder), $lk = 1$ since it has a unit of writhing and no twisting. For a Möbius strip, $Wr = 1$ as a loop and $Tw = \frac{1}{2}$ due to its twist, and therefore $lk = 1\frac{1}{2}$. Similarly, $lk = 2$ for a 2π -twisted 8strip.

Fig. 2(a)–(d) shows scanning electron microscope (SEM) photographs of typical $lk = 1$ samples. (a) is a basic ring or a thin, short cylinder. The disk (b) is a cylinder that grew radially, while the tube (c) grew longitudinally. Some samples with more complex shapes are also categorized as having the $lk = 1$ topology. For example, there are concentric composite cylinders, like (c), and cylinders for which the diameter changes continuously or abruptly (d). Some $lk = 1$ samples have a bowl-like concave surface, as in (d). The typical dimensions of $lk = 1$ samples are 10–300 (around 70 on average) μm in diameter, 1 μm in minimum internal diameter, and 5–600 μm in length. Fig. 2(e) shows an $lk = 1\frac{1}{2}$ material, the so-called Möbius strip, which is famous for its characteristic one-sided, non-orientable surface. Compared to their two-sided counterparts ($lk = 1$ and 2), $lk = 1\frac{1}{2}$ crystals are very rare under any growth conditions. The yield is less than 0.1% of all topological crystals. Fig. 2(f) and (g) shows thin and well-grown $lk = 2$ materials. $lk = 2$ samples have a similar (outer) circumference as $lk = 1$ crystals. On the other hand, they are definitely limited in growth in other directions due to their twisted nature, as demonstrated by sample (g),

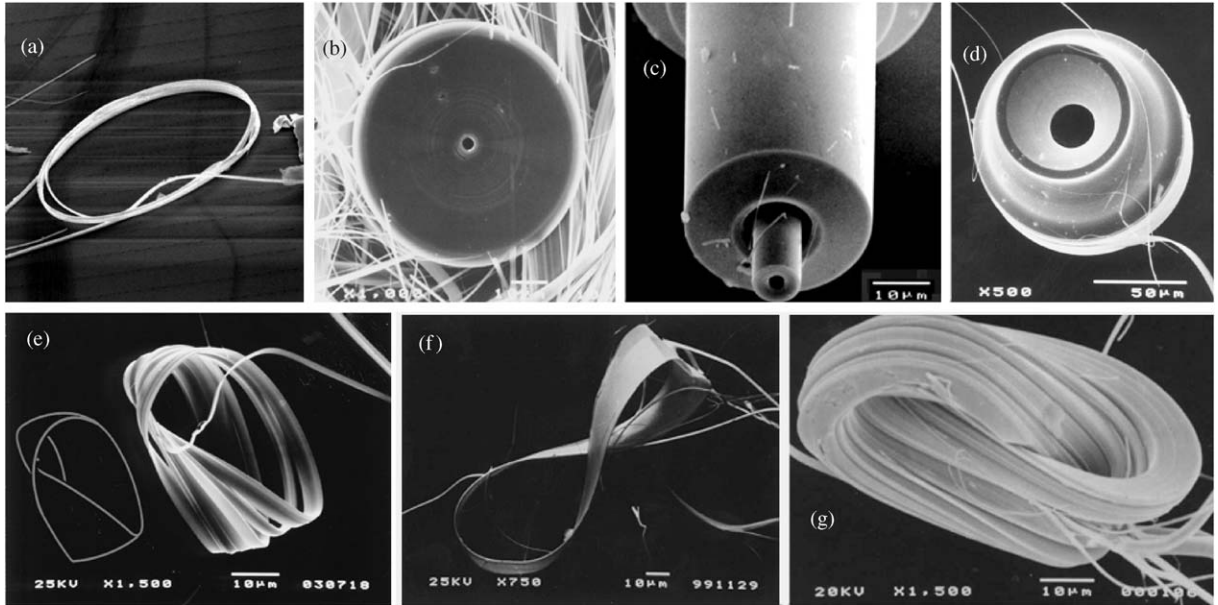


Fig. 2. Scanning electron microscope images of typical topological crystals. (a)–(d) $lk = 1$, (e) $lk = \frac{1}{2}$, (f), and (g) $lk = 2$.

which shows the maximum thickness. Right- and left-handed twists are produced at virtually an equal rate: 82:79 for samples taken from nine batches. $lk = 2$ materials represent an average of 4.2% of all topological crystals when Nb powder is used. However, with Nb rods, this value occasionally is as high as 50–80%, although in other cases it remains in the single digits. The higher-yield batches tend to produce $lk = 2$ samples in a growth region that is separated from that of $lk = 1$ samples. In the ampoule, while a higher-temperature zone, which is about 14 cm long, produced $lk = 1$ and 2 crystals in a ratio of 7:3, the remaining colder zone only produced $lk = 1$ crystals. The direction of the growth of topological crystals varies depending on each sample, as seen in Fig. 2(a)–(c). Disk-, ring- and tube-like cylinders all grow simultaneously in any given batch. Let l , d and t represent the longitudinal length, the outer diameter and the wall thickness of a cylinder. The l/d ratio, a measure of variety in shape, varies more than 400-fold in a single batch. Changes in mean dimensions with time are shown in Fig. 3. While the average t grows constantly, the average l does not increase simply. This indicates that the growth rate of l depends more strongly on each

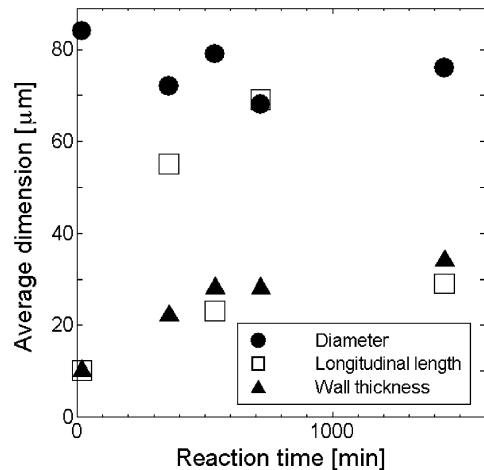


Fig. 3. Average dimensions of $lk = 1$ (cylindrical) topological crystals from a batch with respect to reaction time.

sample. In addition, the outer diameter d gradually decreases with the reaction time.

2.4. Structural properties

NbSe_3 has a quasi-one-dimensional crystal structure based on highly asymmetric atomic bonding. It

is a monoclinic system: space group $P21/m$ with lattice parameters of $a = 10.008$, $b = 3.478$, $c = 15.625 \text{ \AA}$ and $\gamma = 109.4^\circ$ according to PDF 29-4929. Nb and Se atoms combine by strong covalent/metallic bonding to form infinitely long trigonal chains. Chains are aligned along the b -axis and are weakly bonded to each other; more strongly in direction c than in a . This asymmetric atomic bonding is reflected in asymmetry in the electric conductivity, elastic moduli and the growth rate, which is responsible for the shape of the ribbon.

The crystal structure of powdered topological crystals was analyzed by X-ray diffraction (XRD). Fifty rather massive rings were ground in a mortar and then held using adhesive tape. Whiskers from the same growth batch were prepared in the same way. Fig. 4 shows the diffraction angle 2π ($^\circ$) vs. intensity I (count) of rings and whiskers. As

summarized in Table 1, although each diffraction peak for rings shows one-on-one correspondence to those for whiskers, the lattice spacing shows significant deviation from that of whiskers. The lattice parameters of rings were determined to be $a = 9.55$, $b = 3.34$, $c = 15.59 \text{ \AA}$ and $\gamma = 107.1^\circ$ by extrapolation [16]. Those of whiskers were $a = 10.37$, $b = 3.47$, $c = 15.67$ and $\gamma = 109.6$. a , b and c of rings were reduced by 5.1%, 3.6% and 0.2%, respectively. The very large values of strain obtained by the powder method should be treated carefully. Our recent XRD measurements on few individual, untreated samples showed that their strain is not as much as these values. This suggests that ring crystals are plastically deformed by mechanical compression, probably during their formation. The c direction seems to be less affected by rolling of a crystal because it is perpendicular to

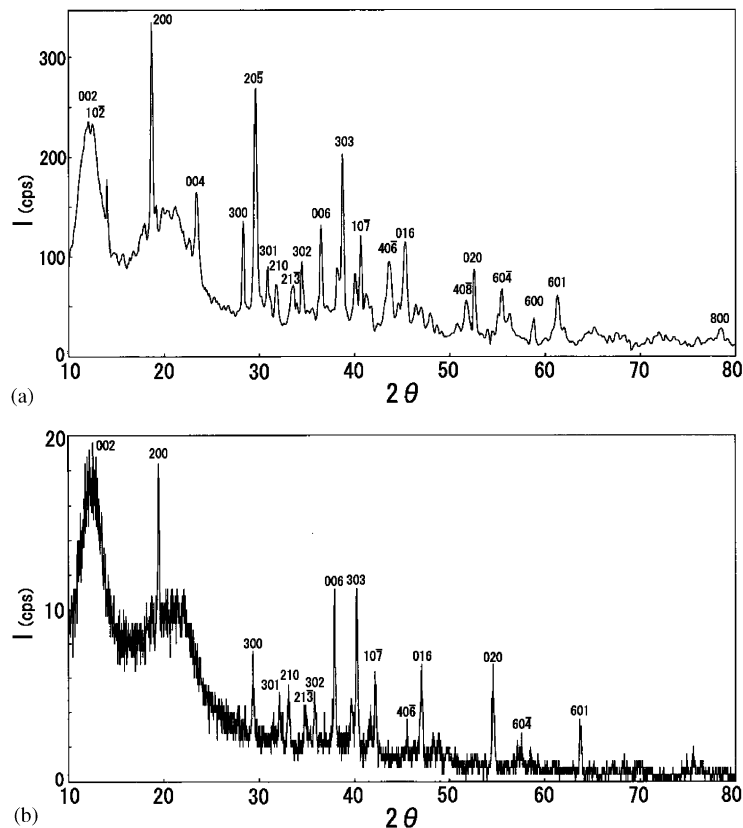


Fig. 4. X-ray powder diffraction ($\text{CuK}\alpha$) pattern of (a) NbSe_3 whiskers and (b) $lk = 1$ topological materials held on adhesive tape. Sample (b) consists of about 50 rather thick topological materials.

the axis of the bending moment so that it remains straight after being rolled. The value of the strain is fairly large even if it is considered that the accuracy of the results is rather low. However, we

Table 1
Main XRD peaks of NbSe₃ whiskers and $lk=1$ topological crystals

Index (hkl)	2π (°)	Whisker		Ring		
		d (Å)	I (%)	2π (°)	d (Å)	I (%)
100	9.20	9.58	53	9.73	9.08	30
002	11.95	7.41	4	12.60	7.02	20
10 $\bar{2}$	12.45	7.11	4	—	—	—
102	17.45	5.08	12	18.13	4.89	10
003	17.85	4.97	17	18.67	4.75	20
200	18.75	4.76	100	19.4	4.57	100
004	23.40	3.80	40	—	*—	—
300	28.30	3.15	39	29.44	3.03	40
20 $\bar{5}$	29.70	3.01	94	—	—	—
301	30.85	2.89	21	32.07	2.79	20
210	31.75	2.82	15	33.06	2.71	20
21 $\bar{3}$	33.45	2.68	15	34.71	2.58	20
302	34.50	2.60	25	35.74	2.51	20
006	36.45	2.46	39	37.88	2.37	90
400	38.10	2.36	21	39.63	2.27	20
303	38.65	2.33	69	40.25	2.24	100
015	40.00	2.25	19	41.73	2.16	10
10 $\bar{7}$	40.80	2.21	35	—	—	—
21 $\bar{6}$	43.55	2.08	26	45.77	1.98	10
016	45.35	2.00	34	47.04	1.93	50
10 $\bar{8}$	47.10	1.93	8	—	—	—
40 $\bar{8}$	51.75	1.77	14	—	—	—
020	52.55	1.74	27	54.55	1.68	60
60 $\bar{2}$	55.45	1.66	20	57.63	1.60	10
600	58.65	1.57	9	—	—	—
601	61.30	1.51	19	63.62	1.46	30
800	81.70	1.18	7	—	—	—

didn't find any evidence of structural breaches or the polycrystalline nature in most topological materials through SEM or transmission electron microscopy measurements. By observing the two characteristic CDW states for $lk=1$ and 2 materials by low-temperature electron diffraction technique and transport measurements, we confirmed that the crystallinity of the topological materials is rather good. In addition, the residual resistance ratio (RRR) of an $lk=1$ material can be as high as 29, while that of a NbSe₃ single crystal synthesized by us has a comparable value, i.e. around 100.

3. Formation and growth mechanism

3.1. Formation of a looped whisker

We found that pre-reacted selenium acts as a template that can bend NbSe₃ whiskers by the force of surface tension. Fig. 5(a) shows a solidified Se droplet and NbSe₃ whiskers taken from a post-quench batch. Some whiskers in the figure cling to the spherical surface of the droplet. Consequently, they form arcs. With further growth, these whiskers could eventually wrap around the droplet. Note that the droplet has a diameter similar to a typical topological crystal. The two ends of a whisker could easily coalesce by loose van der Waals' bonding of NbSe₃ to form a seamless ring. This model is consistent with the fact that topological crystals are produced most efficiently before the reaction and transportation proceed, since it is crucial in this

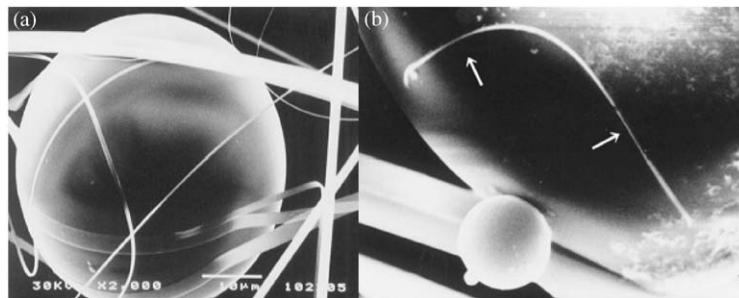


Fig. 5. (a) An SEM micrograph of NbSe₃ whiskers spontaneously rolling around a solidified selenium droplet. (b) An SEM image of a NbSe₃ whisker that has twisted by itself on the surface of a Se drop. It is flipped over at the two points indicated by arrows.

model that a large amount of selenium is left unreacted. This model is particularly important because it implies the possibility of a vapor–liquid–solid (VLS) growth process.

3.2. Generation of a twist in a looped whisker

By adding a twist-generating mechanism to the above theory, we can model the formation of $lk = 1\frac{1}{2}$ and 2 materials. In fact, we have found some whiskers attached to Se, as in Fig. 5(b) that are twisted. Such twisting may originate in the symmetry of the elastic properties of NbSe₃. A twisting deformation requires an internal shear strain. The surface tension of a Se droplet acts on a whisker as a bending force and causes only uniaxial stress. As a monoclinic crystal, however, NbSe₃ has off-diagonal shear components in its elastic compliance matrix, which make the crystal respond to a uniaxial stress with shear strain in addition to uniaxial strain [17]. Therefore, it is possible that a bent NbSe₃ whisker could twist by itself. In this model, a twist would have a continuous pitch that depends on the dimensions of the whisker. Furthermore, a twist would be localized as in Fig. 5(b) to minimize the interface energy with a droplet. In effect, this mechanism generates twists in units of π .

Another possible twist-generating mechanism is premised on over-encirclement. Suppose that a whisker wraps around a droplet twice before its both ends are connected to each other. The resultant form (on the left in Fig. 6) has a writhing number $Wr = lk = 2$. According to White's theorem, the shape is topologically the same as that of the 2π -twisted $lk = 2$ material on the right, i.e. the

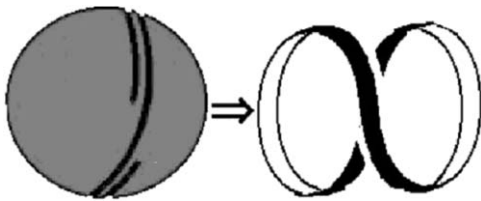


Fig. 6. Schematic diagram of $lk = 2$ topological material (figure-eight strip) in a pristine shape with double-writhing ($Wr = 2, Tw = 0$) as formed by double encirclement (left) and with a twist ($Wr = 1, Tw = 1$) as it is opened afterward.

two shapes can be continuously transformed to each other. Hence, over-encirclement is equivalent to the generation of a twist of 2π . The distribution of the circumference of topological crystals reflects this mechanism. The distribution for 61 $lk = 2$ materials had a peak at around $400\ \mu\text{m}$, which is roughly double that of about $250\ lk = 1$ materials, i.e., $250\ \mu\text{m}$. This supports the above theory because double-encirclement would result in a double circumference. This also suggests that the production of $lk = 2$ materials is mainly due to the double-encircling mechanism. Therefore, the spontaneous generation discussed above is likely to be relevant to only for $lk = 1\frac{1}{2}$ forms. Most $lk = 2$ materials have a twisted shape (Fig. 6, right). This suggests that there is a transition from the initial form of $Wr = 2, Tw = 0$ (Fig. 6 left) to the $Wr = 1, Tw = 1$ form (right). A possible explanation is that transformation from the writhed form to the twisted form occurs due to interaction between the shrinking droplet and a topological crystal.

3.3. Growth mechanism

Assuming the above model, a topological crystal has degrees of freedom about its helicity that cause a large variation in the l/d ratio. When the ends of an encircling whisker connect, a spiral should be formed instead of a perfect circle due to random misalignment. The exposed area at the tips of a whisker (the $\{010\}$ face) is the region for the most efficient growth of the topological crystal. As a consequence, the growth of a topological crystal is dominated by 010 growth along the circumference in a manner that resembles the spiral growth induced by a screw dislocation. As schematically shown in Fig. 7, the helicity of a topological crystal is either “radial” (a), “longitudinal” (b), or intermediate between them. We can simulate the growth of these crystals by assuming the growth rates in the three basic directions **a**, **b** and **c**. For a whisker, we estimate the ratio of these growth rates as 10:1000:1. The same ratio would apply to a topological crystal because asymmetric growth is based on large inhomogeneity in the bonding strength of NbSe₃. In fact, the volume growth rate of a whisker is on the same order ($10^{-15}\ \text{m}^3/\text{min}$) as that of a topological crystal. A simple calculation

demonstrates that the l/d ratio for two extreme cases (Fig. 7(a) and (b)) differs by 1000-fold. This is consistent with the observed wide distribution of this value over 400-fold.

Moreover, we found an indication of the VLS growth of NbSe_3 , which result in the morphology of topological crystals. Fig. 8(a), where NbSe_3 crystallites appear out of a fractured Se drop, demonstrates that NbSe_3 in the atmosphere can accumulate into a Se droplet and crystallize inside. It is quite feasible that a Se droplet can promote the VLS growth of a topological crystal encircling it by supplying NbSe_3 to the area of mutual contact. The higher growth rate of a topological crystal at the internal periphery seems to be a

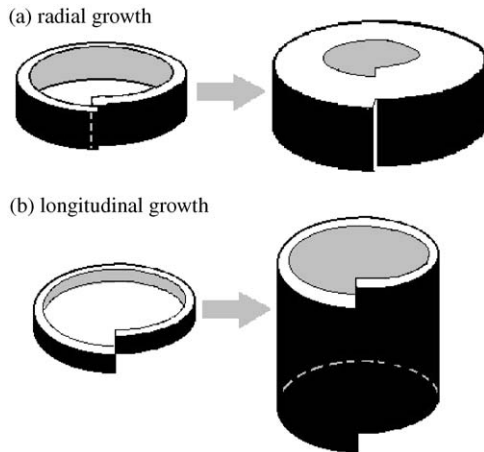


Fig. 7. Schematic diagram of two extreme configurations of a growing NbSe_3 whisker rolled into a helix. Growth would be (a) radial and (b) longitudinal.

consequence of this, since it is in touch with a droplet at the internal periphery. In addition, XRD measurements revealed that topological crystals showed only compression.

If topological crystals only grow inward, any imposed stress would only be compressive. If a Se drop wrapped by a topological crystal could change in size, the resulting growth form would have countless varieties. In most cases, a Se droplet seems to rapidly disappear during growth because very few topological crystals have droplets within the hole. One of few examples is shown in Fig. 8(b). The topological crystal has an hourglass shape possibly because the volume of the enveloped drop has decreased and does not match the circumference of the topological crystal. This shrinkage of a drop could cause the formation of minor varieties like ellipses. Further complex shapes can be formed by the interaction between a change in a drop and the growth of a topological crystal, depending on their respective time scales. The topological crystals in Fig. 2(c) and (d) are possible examples; topological crystals with varying diameter (d), and composite concentric cylinders (c). Moreover, a few topological crystals have a concave, supposedly spherical, surface. This surface is thought to be formed at the interface between a drop and the topological crystal.

4. Discussion

In terms of crystal defects, our topological crystals can be considered to be a physical

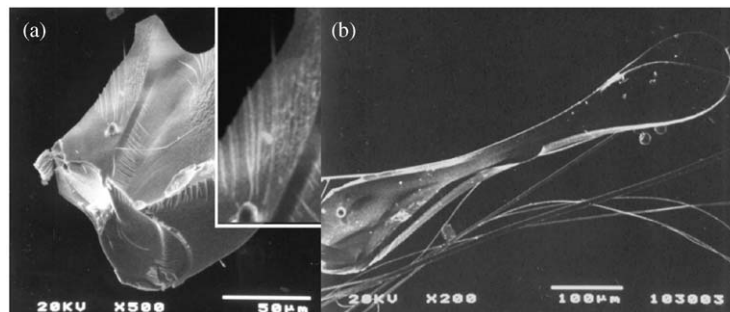


Fig. 8. (a) SEM image of a fractured selenium droplet containing fragmentary NbSe_3 whiskers. (b) SEM image of a $lk = 1$ topological crystal (ring, i.e. a short cylinder) transformed into an hourglass shape due to the surface tension of selenium within the ring.

representation of perfect disclinations [18] and dispirations in crystal solids. In the ideal case of a whisker encircling a drop to form a perfect circle (or twisted circle), all three kinds of topological crystal have a wedge disclination with a power $\omega = +2\pi$. Furthermore, forms $lk = 1\frac{1}{2}$ and 2 also have a twist disclination with Frank vector $\omega = \pm\pi$ and $\pm 2\pi$. If a topological crystal is a helix, it will have a translational defect (dislocation) in addition to a rotational defect (wedge and twist disclinations). These combinations that have the symmetry of a screw are called wedge and twist dispiration.

Both of the two possible types of dislocation (dispiration), global and local [19,20], seem to occur in our materials. A global disclination line virtually pierces the hole of a topological crystal while a localized disclination line is a substantial line defect inside a crystal. A localized disclination in a solid would accompany a planar defect like a dislocation wall or grain boundary to compensate elastic energy. As a consequence, a plastic deformation localizes at the local disclination. The former is seen with thinner materials (less than a few μm), which open elastically if cut and eventually make an almost straight, uniformly curved arc. Initially, they have a virtual global disclination that overlaps their center axis, and afterward the line slips out through the cut point. On the other hand, rather thick materials are formed plastically: such materials retain their initial shapes even when cut. Therefore, their disclinations are localized almost at the center.

The topological equivalence between a wedge disclination (which corresponds to Wr) and a twist disclination (Tw) can only be applied in our materials if they are delocalized. This field of crystallography has not been previously explored due to the rarity of delocalized perfect disclinations, especially twist disclinations, in crystal solids. An open-end tubular system of two-dimensional material could have a global wedge disclination, but would not likely have a twist disclination. NbSe_3 offered an advantage over

tubular systems due to its quasi-one-dimensional nature.

Acknowledgements

The authors are grateful to Prof. Yamaya, late Prof. Sambongi, Dr. Inagaki, T. Toshima and T. Matsuura for stimulating discussions. This study was supported by Grant-in-Aid for Scientific Research (A) and (B), as well as Grant-in-Aid for Encouragement of Young Scientists of the Ministry of Education Culture, Sports, Science and Technology in Japan.

References

- [1] H.W. Kroto, J.R. Heath, S.C. O'Brien, R.F. Curl, R.E. Smalley, *Nature* 318 (1985) 162.
- [2] R. Tenne, L. Margulis, M. Genut, G. Hodes, *Nature* 360 (1992) 444.
- [3] S. Iijima, *Nature* 354 (1991) 56.
- [4] Y. Feldman, E. Wasserman, D.J. Srolovitz, R. Tenne, *Science* 267 (1995) 222.
- [5] A. Loiseau, F. Willame, N. Demoncey, N. Schramchenko, G. Hug, C. Colliex, H. Pascard, *Carbon* 36 (1998) 743.
- [6] D.H. Galván, Jun-Ho Kim, M.B. Maple, E. Adam, *Fullerene Sci. Technol.* 8 (2000) 143.
- [7] M. Hayashi, H. Ebisawa, *J. Phys. Soc. Japan* 70 (2001) 3495.
- [8] S. Tanda, T. Tsuneta, Y. Okajima, K. Inagaki, K. Yamaya, N. Hatakenaka, *Nature* 417 (2002) 397.
- [9] E.N. Bogachek, I.V. Krive, A.S. Rozhavsky, *Sov. Phys. JETP* 70 (1990) 336.
- [10] Y.-S. Yi, A.R. Bishop, *Phys. Rev. B* 58 (1998) 4077.
- [11] Y. Okajima, H. Kawamoto, M. Shiobara, K. Matsuda, S. Tanda, K. Yamaya, *Physica B* 284–288 (2000) 1659.
- [12] A. Meerschaut, J. Rouxel, *J. Less-Common Met.* 39 (1975) 197.
- [13] F. Lévy, H. Berger, *J. Crystal Growth* 61 (1983) 61.
- [14] R.E. Thorne, *Phys. Rev. B* 45 (1992) 5804.
- [15] J.H. White, *Am. J. Math.* 91 (1969) 693.
- [16] J.B. Nelson, D.P. Riley, *Proc. Phys. Soc. London* 57 (1945) 160.
- [17] R.F.S. Hearmon, *An Introduction to Applied Anisotropic Elasticity*, Oxford University Press, London, 1961.
- [18] F.C. Frank, *Philos. Mag.* 42 (1957) 809.
- [19] W.F. Harris, *Surf. Def. Prop. Sol.* 3 (1974) 57.
- [20] A.E. Romanov, V.I. Vladimirov, *Dislocations*, in: F.R.N. Nabarro (Ed.), *Solids* 9 (1992) 191.